Renewable and Sustainable Energy Reviews 21 (2013) 272–287

Contents lists available at SciVerse ScienceDirect

Renewable and Sustainable Energy Reviews

journal homepage: www.elsevier.com/locate/rser

A methodological review to estimate techno-economical wind energy production

Julieta Schallenberg-Rodriguez *

Universidad de Las Palmas de Gran Canaria, Spain

ARTICLE INFO

Article history:
Received 26 September 2012
Received in revised form
7 December 2012
Accepted 10 December 2012
Available online 31 January 2013

Keywords:
Wind
Evaluation
Energy production
Cost
Canary Islands

ABSTRACT

Wind energy represents an important energy source and, even more, it is called to play a crucial role in the future energy supply. In this context, it is crucial to estimate the technical and economical wind energy potential in different regions and areas. This paper includes an extensive review of methodologies proposed by several authors. Based on this review, a set of equations for the evaluation of wind energy production in a given area is proposed, being the input data: mean wind speed and shape factor at any height or even just the mean wind speed. To calculate the wind energy production, wind farm configuration (array efficiency/wake losses) and extrapolation/interpolation of wind speed and shape factor of Weibull distribution to the hub height, have been the main issues discussed. The distances among wind turbines are determined according to economic criteria, where two different approaches have been considered: maximizing income or minimizing cost per kWh. Available wind data usually include mean wind speed and shape factor at certain heights but, very often, not at the hub height. Several methods for extra/interpolation of wind speed and shape factor have been reviewed and a set of equations has been proposed to calculate them at the hub height. A methodology to calculate the annualized wind generation cost (c€/kWh) is also proposed. One of the premises of this methodology has been that calculations should be able to be done simply using calculator and common office software programs. Another premise has been that the methodology proposed is not meant for a detailed evaluation of energy production of one particular windfarm, but to establish a general methodology to study relatively big areas, like islands or whole regions. A practical application of the methodology proposed has been carried out using wind data from the Canary Islands.

Contents

* Tel.: +34 928451936.
E-mail addresses: jschallenberg@dip.ulpgc.es, julieeta.schallenberg@gmail.com

1364-0321/$ - see front matter © 2013 Elsevier Ltd. All rights reserved.
http://dx.doi.org/10.1016/j.rser.2012.12.032

1. Introduction

Wind energy represents nowadays a relevant electricity production technology in some countries (e.g. in Denmark, wind power accounted for 24% of domestic electricity production in 2011—the highest figure in Europe—; in Spain the wind contribution was 16% in 2011) and, even more, it is called to play a crucial role in the future energy supply worldwide and in the European Union. In the year 2011, the worldwide wind capacity reached 237 Gigawatt (GW). This wind capacity can provide 500 Terawatt-hours (TWh) per annum, around 3% of the global electricity consumption [1]. The market for new wind turbines reached a new record: 40 GW were installed in 2011, 6% more than in 2010. Since many years the wind industry has been driven by the Big Five markets, being their installed capacity by the end of 2011: China (63 GW), USA (47 GW), Germany (29 GW), Spain (22 GW) and India (16 GW). They have represented the largest share of the increase in wind power during the last two decades; accounting, by the end of 2011, to 74% of the worldwide wind capacity [1]. The wind capacity installed by the end of 2011 in the European Union (EU) was 94 GW, enough to supply 6.3% of the EU's electricity [2]. The World Energy Association [1] expects an installed wind capacity of 500 GW by 2015 and 1000 GW by 2020. In Europe, the European Wind Energy Association expects 230 GW to be installed by 2020 [3].

In this context of wind development, it is crucial to estimate the technical but also economical wind potential in regions and areas. There are some authors that have assessed or proposed a methodology to partially or fully evaluate the wind energy potential production in a given area and, in some cases, they have also included an economical assessment [4–13]. There are also some software programs to evaluate the wind energy production and some economical parameters. This paper includes an extensive review of the methodologies proposed by several authors and, based on this review, a novel set of equations for the evaluation of the potential wind energy production in a given area is proposed. A simple method to evaluate the economical assessment is also proposed. The methodology used in this paper is explained in the next paragraph.

2. Methodology

The aim of this paper is to propose a methodology to calculate the techno-economical wind energy potential production in a given area. The methodology is based on a detailed literature review. One of the premises of the methodology proposed has been that the calculations should be able to be done simply using pen, paper and calculator and common office software programs (no specific software program should be needed). Another premise has been that the methodology proposed is not meant for a detailed evaluation of the energy production of one particular windfarm at one particular site, no micrositing study is proposed, but to establish a general methodology to study a relatively broad area, like an island or a whole region. The wind data that need to be available to implement this methodology should include the mean wind speed and the shape factor of the Weibull distribution, k, at any different heights.

The first step of the methodology is to determine the wind farm configuration (Section 3). The wind farm configuration depends on the wake effect, which determines the array losses. Wind farms take a matrix form where the array efficiency is proportional to the inter-turbine and inter-row spacing. The determination of these distances should be done according to economic criteria, where two different approaches may be possible: maximizing the income or minimizing the cost per kWh. Once the wind farm configuration (understanding as such the downwind and crosswind distances) has been determined, the wind turbines are located on the area to be studied. The configuration chosen will determine the number and location of each wind turbine.

The next step is to calculate the wind energy production (Section 4). As starting point, the wind turbine that wants to be installed has to be selected. Then the wind turbine power curve and the wind data (mean wind speed and shape factor, k, at the hub height) are used to calculate the wind energy production. Wind atlases usually provide the mean wind speed and the shape factor, k, at certain heights but, very often, not at the hub height. That is why several methods for the extra/interpolation of wind speed and shape factor have been reviewed and a set of equations has been proposed to calculate the mean wind speed and the shape factor at the hub height when both parameters are available at different heights.

The last step is the calculation of the generation cost (c€/kWh) of the wind energy that could be installed in the selected area (Section 5). To display the annualized generation cost, the cost-resource curve has been utilized. This section includes also a detailed review and analysis of the investment and operation and maintenance (O&M) costs.

3. Wind farm configuration

3.1. Array losses and wake effect

Let us consider that a given area wants to be exploited from the wind energy point of view. The next step would be to optimally

locate the wind turbines within this available area. Wind farms take a matrix form where the array efficiency (η_{ar}) is proportional to the inter-turbine and inter-row spacing, which are function of the rotor diameter. The array efficiency is the efficiency of the whole wind farm, which decreases with closer spacing due to the interference of wind turbines.

An operating wind turbine reduces the wind's speed for some distance downwind the rotor. If the turbines are located too closely, they will interfere with each other, reducing the energy output of those downwind. The array efficiency is the actual output of clustered turbines compared to the one that would be obtained without interferences. The array efficiency depends on the spacing between turbines and the nature of the wind regime [10]

$$\eta_{ar} = \frac{Annual\ energy\ whole\ array}{Anuual\ energy\ one\ iolated\ turbine\, number\ of\ turbines} \quad (1)$$

The array losses are mainly functions of [4]:

- Wind turbine spacing
- Wind turbine operation characteristics
- Number of turbines and size of the wind farm
- Frequency distribution of the wind direction

Array losses can be reduced optimizing the geometry of the wind farm. Different distributions of turbines sizes, the overall shape, the size of the wind farm and turbine spacing within the wind farm, all affect the degree to which wake effect reduces the energy capture [4].

In the near-wake zone, the wake expands until the pressure in the wake reaches the ambient level, probably 2–3 rotor diameters (*D*) downwind. From the near-wake out to approx. 5–6*D*, additional turbulence is mainly generated by the radial flow shear, dissipation starts to drain turbulent energy and the width of the wake increases and, during this process, the speed deficit is reduced. The vertical profile of wake-generated turbulence in the wake is not symmetric, but has a maximum somewhat above hub height [14].

Extensive theoretical and wind-tunnel studies indicate that, under typical conditions, interferences increase quite rapidly when turbines are less than 10 rotor diameters (10*D*) apart. For an infinite number of turbines with 10*D* spacing, the array efficiency would be ca. 60%. But, for a finite number of wind turbines, average losses are much lower and closer siting is practical [10]. Table 1 shows estimated efficiencies of square arrays as a function of turbine spacing and array size, being *D* the rotor diameter.

Other authors suggest other values for the array efficiency as a function of the distances down- and crosswind.

As per [15], for turbines that are spaced 8 to 10*D* apart in the prevailing downwind direction and 5*D* apart in the crosswind direction, array losses are typically less than 10%.

Table 1
Array efficiencies for different sizes and spacing of square wind farms.
Source: [10].

Array size	Turbine spacing					
	4D	5D	6D	7D	8D	9D
	Array efficiency (%)					
2 × 2	81	87	91	93	95	96
4 × 4	65	76	82	87	90	92
6 × 6	57	70	78	83	87	90
8 × 8	52	66	75	81	85	88
10 × 10	49	63	73	79	84	87

According to [11], the wind speed losses are less than 10% for downwind distances between 6 and 10*D* and crosswind distances between 2 and 3*D*. In regions where the predominant wind-direction is one, the turbines can be located quite close.

For [6], a turbine spacing of 8 to 10 rotor diameters in the prevailing wind direction (downwind) and 3 to 5 rotor diameters across the main wind direction (crosswind) represents reasonable array geometry. Under such conditions, the array efficiency reaches approximately 90%. This result has also been confirmed by practical experiences. They also claim that, on a real site, the array efficiency is always less than 100%, as the mutual aerodynamic interference is noticeable at distances of up to 20 rotor diameters or more.

For infinite clusters, most models agree well. It is expected that turbulence—when the roughness elements are wind turbines—will be in balance much sooner than the mean wind speed. But, how far into the cluster is this point of balance reached? It is stipulated that this happens when wakes merge so that there is no reminiscence of ambient-flow between units. Depending on the specific geometry, the distance in terms of wind turbine rows would be of the order 5–10, corresponding to 3–5 km with contemporary wind turbine sizes [14].

Array efficiency depends on the distance among wind turbines and the number of wind turbines rows (see, e.g., [10,14]). [14] compared their model to other models using a wind farm configuration of 7 × 7*D* and varying the number of rows. They concluded that: for an infinite number of wind turbines rows, the efficiency is 42% (other models result in efficiencies between 38–42%), for 15 wind turbines rows the efficiency is 80% (other models result in efficiencies between 50 and 83%) and for 10 wind turbines rows the efficiency is 85% (other models result in efficiencies between 64 and 88%).

[16] suggested the following relation between efficiency and spacing:

Downwind:

$$PR_D:\ 0.012 \cdot (12-d)^2 \quad (2)$$

$d \in (4D,\ 12D)$

Crosswind:

$$PR_C:\ 1-0.25 \cdot d \quad (3)$$

$d \in (0,\ 4D)$

where PR: Power reduction, *d*: distance/*D*.

For example, in the case of downwind distance of 10*D*, the PR_D will be 4.8%; and in the case of downwind distance of 12*D*, the PR_D will be 0%. In the case of crosswind distance of 4*D*, the PR_C will be 0%.

But not only the number and distance among wind turbines are important in order to determine the array efficiency, also the wind direction distribution plays an important role. Unidirectional or bidirectional winds allow for closer crosswind spacing [10].

Another factor to be taken into account is the rate at which the wind energy extracted by a turbine is replaced with energy from winds above, which depends on the vertical wind profile and on the mixing between layers [10]. The extraction of energy from the wind results in an energy and velocity deficit, compared with the prevailing wind, in the wake of wind turbines. The energy loss in the turbine wake will be replenished over a certain distance by exchange of kinetic energy with the surrounding wind field. The extent of the wake in terms of its length as well as its width depends primarily on the rotor size and the power production. The momentum and energy exchange between the turbine wake and the prevailing wind is accelerated when there is higher turbulence in the wind field, reducing the array losses [4]. Thus, in the case of stratified thermal winds, characterized by a small

increase of wind-speed with height and little mixing between layers, the disturbance is carried far downwind and the interference between wind turbines is much higher than expected [10].

The design of the wind farm requires careful consideration of these effects in order to maximize the energy capture. Closer spacing of wind turbines may allow more wind turbines on the site, but will reduce the average energy capture from each turbine in the wind farm [4].

The exact calculation of array losses requires knowledge of the location and characteristics of the turbines located in the wind farm, knowledge of the wind regime and appropriate models of turbine wakes to determine the effect of upstream turbines on downstream ones. A number of turbine wake models have been developed; which can be categorized as [4]:

- surface roughness models;
- semi-empirical models;
- eddy viscosity models;
- full Navier–Stokes solutions.

Due to the big number of variables to be taken into account, the tendency nowadays is to study the wake effect of wind farms using tools as numerical models, heuristic methods (e.g. [16]) artificial neural networks and, lately, genetic algorithms (e.g. [17–20]).

In the Canary Islands the prevailing winds are the tradewinds, which are predominantly unidirectional winds. This suggests that the wind turbines downwind, but specially crosswind, could be placed closer, being the array efficiency higher than the suggested average standards for the selected configuration. A study of the micrositing of each wind farm that would locally optimize the turbine layout is out of question for a general study at large scale (e.g. island, region). If the study is carried out for one particular wind farm, a micrositing analysis should be carried out. Therefore, if the targeted area is a whole region, even taken into slightly consideration the general characteristics of the local winds (e.g. tradewinds in the Canary Islands, which are known for being the steadiest wind system in the lower atmosphere [12]), a common spacing down- and crosswind has to be chosen for all wind farms and a general array efficiency has to be calculated for the configuration chosen.

This simplified solution is the feasible one when local wind conditions (at site level) and the number of turbines within a wind farm are not taken into account, since a local study of each wind farm cannot be considered for a general study, as a regional one. Therefore, one should distinguish two different cases: analysis of one wind farm (or several wind farms), where a micrositing analysis should be carried out, and general studies (e.g. regional level, big areas with too many wind farms to carry out an individual analysis), where a common configuration is selected to generalize the analysis, losing accuracy but making it more feasible.

One criterion to be taken into account when selecting the wind farm configuration is the economic criterion. There may be two different approaches: maximizing the income or minimizing the cost per kWh. In the first case, one would try to maximize the income of one particular piece of land where the wind farm should be installed, trying to install a big number of turbines in a limited plot but keeping also in mind the array efficiency criterion. In this case, the array efficiency will not be the highest possible but the global electricity production will be higher (although the individual electricity production per wind turbine will be lower). In the second case, one would try to maximize the output of each single wind turbine, maximizing the efficiency of each generator and, consequently, the array efficiency and minimizing, therefore, the generation cost per kWh (c€/kWh). In this case, less wind turbines will be installed since the distances between wind turbines will be higher, obtaining less electricity production from the plot but a higher return for each euro invested in wind turbines. Fig. 1 illustrates both situations, the left side of the figure shows a low array efficiency configuration, many wind turbines in a given area and, therefore, short distances among them; the right side shows a high array efficiency configuration, meaning less wind turbines and larger distances among them.

The wind farm configuration selected, in this study, has a downwind distance of 12D and a crosswind distance of 4D. These distances are indeed big but this configuration seeks for the minimum generation cost (being quite conservative according to other authors' opinions). In fact, substituting in the Eqs. (2) and (3) proposed by [16], the result is an array efficiency of 100%. Array efficiencies of 100% are theoretical, since they cannot be reached in clustered wind turbines, but this result gives an indication that this configuration leads to very high array efficiency, approaching 100%. These values are also in line with other authors' opinions.

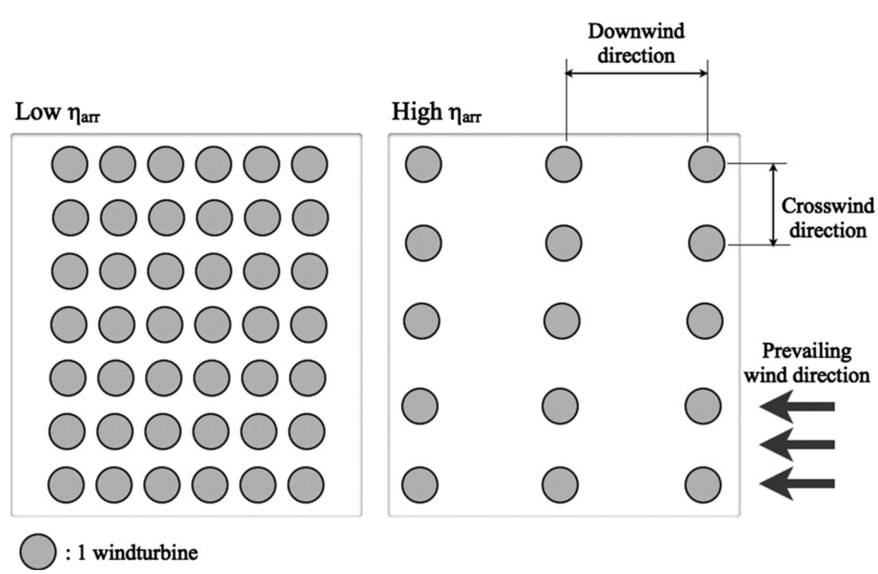


Fig. 1. Array configuration: low (left side) and high (right side) array efficiency depending on the wind turbines layout.

3.2. Location of the wind farms

Once the available areas have been selected and the wind farm configuration has been decided ($12D \times 4D$), the wind turbine to be installed has to be selected in order to obtain the rotor diameter, which is directly proportional to the inter- and intra-array distances. The reference wind turbine (WT) selected for in this case is a 2 MW one with a hub height of 78 m and a rotor diameter of 87 m. This means that the distance between wind turbines in the downwind direction is 1044 m and in the crosswind is 348 m. In other words, the wind farm takes a matrix form where the distance among rows is 1044 m and among columns is 348 m. The wind turbines are then placed in the available areas following the selected matrix form until these areas are filled out with wind turbines.

3.2.1. Wind power density considerations

Another parameter, which is usually used in other studies, is the wind power density referred to the available surface. In some studies the wind energy production is calculated as the product of the wind power density and the total suitable surface. The wind density takes different values depending on the study: 4 MW/km^2, worldwide scale [9] and state scale [21]; 3 MW/km^2, Europe [22] or 8 MW/km^2, also for Europe [3]. This method is commonly used in studies where the territorial scope is quite big. However, in a more detailed study, where the scale is also smaller, an analysis as the previous one is needed in order to locate the wind turbines and calculate their energy production.

3.2.2. Wind power saturation

The *saturation wind power potential* is the maximum wind power that can be extracted upon increasing the number of wind turbines over a large geographic region. Increasing the number of wind turbines worldwide allows energy extraction relatively proportional to the number of turbines until saturation is reached. Saturation occurs when sources of kinetic energy at nearby altitudes and creation of kinetic from potential energy are exhausted. At saturation, each additional turbine still extracts energy, but that extraction reduces energy available to other turbines, so the average extraction among all turbines decreases to maintain a constant *saturation wind power potential*. At the *saturation wind power potential*, winds still occur because individual turbines can extract no more than 59.3% of the kinetic energy in the wind (Betz's limit) [13].

[13] concluded that, up to about 715 TW (1.4 W/m^2) of installed power at world scale, the output from power-extracting wind turbines increases linearly. At higher penetrations, power output increases with diminishing returns until it reaches global saturation at about 2870 TW installed (5.65 W/m^2). Higher penetrations of wind serve no additional benefit. Thus, for the first 715 TW installed, output increases roughly linearly proportionally to turbine installation, but thereafter, it increases with diminishing returns until saturation. The crossover point is at an installed density of approximately 2.9 W/m^2. It is not necessary to spread turbines evenly across such land. In fact, individual farms can have installed densities of 5.6–11.3 W/m^2 so long as reasonable spreading between farms occurs and the average installed density within and between farms is $\leq$2.9 W/m^2.

Thus, spreading wind farms out worldwide in high-wind locations will increase wind farm efficiency and reduce the number of farms needed compared with packing wind farms side-by-side. The careful siting of wind farms will minimize costs and the overall impacts of a global wind infrastructure on the environment [13].

This saturation effect has to be taken into account when regional studies are developed. Therefore, the resulting wind power density has to be calculated and, if it reaches critical values from the saturation point of view, wind farms have to be spread out or even, in some cases, the number of turbines has to be reduced.

4. Wind energy production

4.1. Methodological considerations

There are several methods to try to estimate the wind energy production. One possibility is to establish the wind turbine to be installed as starting point. Then the characteristic power curve of this particular wind turbine is used to determine the energy production as a function of the wind distribution on-site. This type of methodology is commonly used to calculate the energy production. This is also the method proposed in this case. The reference wind turbine (WT) selected is a 2 MW one (hub height: 78 m, rotor diameter: 87 m).

4.2. Wind data

The next step is to analyze the wind data that are available or can be obtained. Very often wind speed and shape factor of the Weibull distribution, k, are available for different heights. This is the case, for example, in the Canary Islands. For these islands the wind atlas provided by the Instituto Tecnológico de Canarias offers data at grid scale 100×100 m^2. The wind atlas includes mean annual wind speeds and shape factors of the Weibull distribution, k, for each grid cell at an altitude of 40, 60 and 80 m, as well as the predominant wind direction.

The wind atlas of the Canary Islands has been developed using meso- and a microscale models that have been used worldwide since years successfully. The results of the model have been compared to available wind measurements from different met-towers; adjusting the results when necessary. Therefore, even if the wind data of this atlas are not measured data, they are considered to be highly reliable and will, therefore, be treated in this study as actual data.

4.3. Selection of the method to determine the wind production

To select the method to be used, the first step is to analyze the wind data that can be obtained. Depending on the available data, there are different methods to determine the turbine production, as the followings [4]:

- direct use of data over a time interval;
- the method of bins;
- development of velocity and power curves from data;
- statistical analysis using summary measures.

In order to utilize the three first methods mentioned, time series of measured wind data at the desired location and height are needed [4].

Taking into account the available data, average wind speed and k shape factor of the Weibull distribution, which is a common way to express wind data, the method to be used is the statistical analysis.

4.3.1. Commonly used probability distributions

Two probability distributions are commonly used in wind data analysis:

1. the Rayleigh distribution
2. the Weibull distribution

The Rayleigh distribution uses one parameter: the mean wind speed. This means that, when the only parameter that is available

is the wind speed, the Rayleigh distribution is the one that has to be used.

The Weibull distribution is based on two parameters, the mean wind speed and the *k* shape factor, and, thus, can better represent a wider variety of wind regimes [4]. The Weibull distribution function assumes different shapes depending of the value of *k*, the shape factor. When *k* is equal to 2, it becomes the Rayleigh function [23].

4.4. The Weibull distribution as a mean to obtain turbines' annual production

For statistical analysis, a probability distribution is an expression that describes the likelihood that certain values of a random variable (such as wind speed) will occur. Typical probability distributions are the probability density function and the cumulative density function. The probability density function, $p(v)$, describes the frequency of occurrence of winds speeds. The cumulative distribution function, $F(v)$, represents the time fraction or probability that the wind speed is smaller than or equal to a given wind speed value.

In the Weibull distribution, the variations in wind velocity can be described by these two functions:

(1) the probability density function [4,24,25]

$$p(v)=\left(\frac{k}{c}\right)\cdot\left(\frac{v}{c}\right)^{k-1}\cdot\exp\left[-\left(\frac{v}{c}\right)^{k}\right] \quad (4)$$

where k: shape factor of the Weibull distribution, c: scale factor of the Weibull distribution, v: wind velocity.

(2) and the cumulative distribution function [4,5,8,25]

$$F(v\le v_i)=1-\exp\left[-\left(\frac{v_i}{c}\right)^{k}\right] \quad (5)$$

This cumulative distribution function (Eq. 5) represents the probability that the wind speed is smaller than or equal to a given wind speed, v.

Other authors represent the cumulative distribution function as the complementary equation of Eq. (5): $F\,(v\ge v_i)$ [11,23]. This cumulative distribution function represents the probability that the wind speed is larger than or equal than a chosen value, v.

The probability that the wind speed lies between two values (v_1 and v_2) is expressed by Eq. (6) [26]:

$$P(v_1\le v\le v_2)=\exp\left[-\left(\frac{v_1}{c}\right)^{k}\right]-\exp\left[-\left(\frac{v_2}{c}\right)^{k}\right]. \quad (6)$$

4.4.1. Annual energy yield

The calculation of the annual energy yield of a wind turbine at a given site requires the power curve of the turbine and the frequency distribution of the wind speed at the hub height on the site. In order to proceed with the calculations, the cumulative frequency distribution is divided into intervals (bins) and the mean generated power is read off the power curve in the corresponding interval [6]. There are two ways to decide the size of the interval:

- fixed interval size (independently of the interval size used in the power curve)
- to fix the interval size according to the interval provided in the power curve

In the first method, the interval is fixed in advance, e.g. 0.5 m/s, and then the power curve table is consulted. If the interval size in the power curve table is bigger, e.g. 1 m/s, then the values in between have to be interpolated in order to get the wind speed values each 0.5 m/s. This method is often used if calculations are done for a broad numbers of wind turbines (power curves for different wind turbines differ often in their interval size) and one wants to develop standard calculations for all the machines.

In the second method, the interval size is the same as the one provided by the power curve table of the selected machine.

This second method is the one proposed in this paper and, in this case, the interval size chosen is $\Delta v=1$ m/s.

The annual energy yield can be obtained as [6,11]:

$$E=\frac{8760}{100}\cdot\sum_{v_E}^{v_A}P\cdot F(v) \quad (7)$$

where P: power output (kW); $F(v)$: cumulative wind frequency distribution (%); v_E: cut-in wind speed; v_A: cut-off wind speed.

The annual energy yield is then calculated by adding, from v_E (cut-in wind speed) to v_A (cut-out wind speed), the power output corresponding to a wind velocity interval, according to the wind frequency distribution in this interval. The annual energy yield is the integral of power over time.

Eq. (7) can also be expressed as

$$E=8760\cdot\sum_{j=v_E}^{v_A}P(v_j)\cdot\left[F\left(v_{j-\frac{s}{2}}\right)-F\left(v_{j+\frac{s}{2}}\right)\right] \quad (8)$$

where $P(v_j)$: power output for the velocity j, values from the power curve (kW); s: size of the velocity interval selected ($s=\Delta v$); $F(v_{j-s/2})$: cumulative wind distribution for velocity $j-s/2$ (m/s); $F(v_{j+s/2})$: cumulative wind distribution for velocity $j+s/2$.

$F(v_{j-s/2})$ and $F(v_{j+s/2})$ are calculated from Eq. (5). Eq. (5) utilizes two parameters of the Weibull distribution: the shape factor, k, and the scale factor, c. The scale factor is very often not one of the data included in wind atlases or wind databases, which usually include just the shape factor and the mean velocity. But the scale factor can be calculated from the mean velocity and shape factor using [4,25]

$$c=\frac{v}{\Gamma(1+\frac{1}{k})} \quad (9)$$

where v: mean velocity at hub height (m/s), k: shape factor at hub height, $\Gamma(x)$: gamma function

Substituting Eqs. (5) and (9) in Eq. (8), the annual energy production for a particular location (x,y) at the hub height can be calculated as

$$E=8760\cdot\sum_{j=v_E}^{v_A}P(v_j)\cdot\left\{\exp\left[-\left(\frac{\left(v_{j-\frac{s}{2}}\right)\cdot\Gamma\left(1+\frac{1}{k_{x,y}}\right)}{v_{x,y}}\right)^{k_{x,y}}\right]-\exp\left[-\left(\frac{\left(v_{j+\frac{s}{2}}\right)\cdot\Gamma\left(1+\frac{1}{k_{x,y}}\right)}{v_{x,y}}\right)^{k_{x,y}}\right]\right\} \quad (10)$$

where $v_{x,y}$: mean velocity at point x; y at hub height (m/s); $k_{x,y}$: shape factor at point x, y at hub height.

Eq. (10) can be used to calculate the annual energy production of a given wind turbine in a given site. However, there are some simplified methods that can also lead to very good results. [27] proposed a formula (Eq. (11)) that, assuming a Rayleigh distribution, calculates the annual wind energy production when the only known parameter is the mean speed at the hub height

$$E=8760\cdot P_R\cdot\left(0.087\cdot v_{x,y}-\left(\frac{P_R}{D^2}\right)\right) \quad (11)$$

where P_R: rated power of wind turbine (kW); D: diameter of wind turbine (m).

For a detailed derivation of Eq. (11), see [27].

4.4.2. Comparison of annual energy yield

The annual wind energy production of the Canary Islands has been calculated using both equations, Eqs. (10) and (11), in order to compare the results using both methodologies. Table 2 shows the difference when comparing both methodologies for each island. This difference is computed as a percentage and is named "error". Table 2 shows also the number of wind turbines (2 MW each) installed in each island that have been used for calculations.

Although the overall regional error is very small (0.12%), the error varies between islands, moving from 3.39% to 0.52%, being these values also relatively small. Note that the errors compute by island are relative errors, sometimes the production calculated according to Eq. (11) was higher than the one computed according to Eq. (10), and vice versa; that is why the regional error resulted in such a small amount (counteracting effect). However, the errors computed for single turbines show a much higher range, being in some cases higher than 25% (worst case scenario) while in other cases the error was 0.01% (best case scenario).

Shape factors versus error values were also studied to search for possible patterns, but they could not be established. The two extreme error ranges were studied: errors lower than 0.5% and errors higher than 20%. And, although sites with shapes factors near to two (a shape factor of 2 corresponds to the Rayleigh distribution) seem to have a slight tendency to show lower error values, no pattern could really be established. Some sites that had relatively high shape factor values (e.g. 2.7) showed errors lower than 0.5% while other sites with lower shape factors (e.g. 2.4) showed errors higher than 20%.

In conclusion, when using Eq. (11) results will improve when the targeted area and number of wind farms increase. For large studies, as regional ones, results will be quite accurate, being the error quite insignificant. But for site-specific studies, targeting small areas or small number of wind turbines, a more precise formulation, that takes into account the shape factor, is advisable.

4.5. Extrapolation/interpolation of wind speed at different altitudes

4.5.1. Wind speed at high altitudes

Since instantaneous wind energy is proportional to the cube of instantaneous wind velocity, it is important to accurately estimate the wind velocity at hub height by extrapolating wind velocity from relatively lower height.

Among all uncertainty factors affecting the wind power assessment at a site, wind speed extrapolation is probably one of the most critical ones, particularly when considering the increasing size of modern multi-MW wind turbines, and therefore of their hub height [28]. The planetary boundary layer can be considered to consist on a number of layers, each governed by a different set of flow parameters. Wind speed does not increase with height indefinitely; usually there is a wind speed decrease when the altitude reaches ca. 450 m. The wind speed at 450 m height can be four to five times higher than the one near to the ground surface [29].

It is essential for wind power developers to accurately know the wind speed characteristics at the hub-height (usually between 60 to 100 m) and across the rotor because these characteristics determine the turbine's potential electricity production, and therefore the economic feasibility of a candidate wind turbine site. Wind speed and direction at high heights can be measured by: (1) remote sensing, such as collecting SODAR (SOnic Detecting And Ranging) or LIDAR (LIght Detecting And Ranging) data, or (2) installing tall (60 to 100 m) meteorological towers (met towers). Although remote sensing and tall towers are the most accurate methods of measuring wind-shear at a candidate wind turbine site, they are more expensive than installing a standard met tower (40 to 50 m heights, sometimes even lower to 10 m) and then using wind-shear models to extrapolate for estimates of wind speeds at the desired hub-heights. The use of wind-shear models, however, introduces additional uncertainty into the wind resource estimate [30].

Wind shear is defined as the change in horizontal wind speed with a change in height [31]. Wind profile (or wind shear) in the first hundred meters is highly affected by the site where measurements are made, as it depends on wind speed, atmospheric stability, terrain type (and thus surface roughness), the height interval, temperature, season of the year, etc. [12]. In particular, wind shear is strongly affected by atmospheric stratification, and therefore it varies noticeably through time, i.e., hour of the day and month/season of the year as well as from one year to another [12,32,33]. Over the years, different methods have been developed to extrapolate wind speed in the lower atmosphere, assuming that wind profile follows either a power, a logarithmic or a log-linear law.

4.5.2. Methods to calculate wind speed profiles

4.5.2.1. The log-linear law (Log LL). Based on the Monin–Obukhov similarity theory, the Log LL is a physical model stating that the wind velocity at a determined height, v_2, can be calculated as [34]

$$v_2 = \left(\frac{u^*}{K}\right) \cdot \left[\ln\left(\frac{h_2}{z_0}\right) - \psi_m\left(\frac{h_2}{L}\right)\right] \tag{12}$$

where u^*: friction velocity (m/s); K: von Karman's constant (typically 0.4); z_0: roughness length (m); L: Monin–Obukhov stability length (m); h_2: height 2, where the wind speed wants to be determined (m); ψ_m: atmospheric stability function.

The roughness length, z_0, is an empirical parameter that characterizes the influence of surface irregularities on the vertical wind speed profile. The rougher the terrain the thicker will be the affected layer of air and the more gradual will be the velocity increase with height. In the absence of experimental data, z_0 has to be selected on the basis of visual inspection of the terrain [12]. There are reference tables that tabulate the roughness length, z_0, as a function of the terrain type (e.g. see [4,11,12,35]). Some typical values of the roughness length are, e.g., in cities with very tall buildings: z_0=3.0; outskirts of towns: z_0=0.4; for crops or tall grass: z_0=0.05; calm open see: z_0=0.0001.

The stability of the atmosphere is governed by the vertical temperature distribution resulting from radiative heating or cooling of the earth's surface and the subsequent convective mixing of the air adjacent to the surface. Atmospheric stability states are classified as stable, neutrally stable or unstable. These states are important to model the wind vertical profile because of the different amounts of atmospheric mixing which characterized each state [12].

The Log-linear Law has its origin in boundary layer flow in fluid mechanics and in atmospheric research [4]. The Log LL is valid over large ranges of altitude and incorporates the phenomenon of atmospheric stability [12].

Table 2
Comparison of annual wind energy production.

Island	Number of installed turbines	Error (%)
El Hierro	29	0.52
Fuerteventura	1365	1.40
Gran Canaria	448	1.84
La Gomera	53	3.39
La Palma	58	3.25
Lanzarote	384	2.60
Tenerife	194	0.59
Total	2531	0.12

4.5.2.2. The logarithmic law (Log L). In the case of neutral stability ($\psi_m=0$), the Log LL can be simplified to the well-known and widely used logarithmic profile [35]

$$v_2 = \left(\frac{u^*}{K}\right)\cdot\left[\ln\left(\frac{h_2}{z_0}\right)\right] \quad (13)$$

Eq. (13) can also be re-formulated as [4,11,26,28]

$$v_2 = v_1\cdot\frac{\ln(h_2/z_0)}{\ln(h_1/z_0)} \quad (14)$$

This last equation of Log L, which only depends on z_0, is valid only near to the ground: altitudes of 30–50 m, over relatively flat terrain, but not over complex and rough terrain [28].

The friction velocity can be calculated from measurements of wind speed at two (or more) heights from Eq. (13) [36]:

$$v_2 - v_1 = \left(\frac{u^*}{K}\right)\cdot\left[\ln\left(\frac{h_2}{h_1}\right)\right] \quad (15)$$

The friction velocity should be more independent of the absolute wind speed, and would, therefore, allow more inter-comparison and transferability between different heights and locations. The use of the friction velocity to assess wind shear should reduce inconsistencies in the heights at which the observations are taken and negate any bias in the shear parameter due to smaller wind speeds [36]. The theory of wind shear near the surface suggests that variations in the profile of wind velocity with height are dependent on the turbulence profile. The turbulence creates friction between atmospheric layers and greater friction reduces the difference between velocities at different heights and the wind shear is smaller. For turbulence generated by surface roughness a standard wind profile through the boundary could be assumed for that location based on the surface roughness. However, wind shear is not a simple process and has a number of contributing factors each of which can vary significantly in time. The general assumptions are that the wind speed reduces to zero at the surface and there can exist a surface layer within which there is great surface-induced turbulence and small wind shear. For a complex surface one might expect a shallow layer of small wind shear above which there would have to be a layer of large wind shear for the transition to the geostrophic wind at the top of the boundary layer [36].

4.5.2.3. The power law (PL). Since the use of the Log LL is complex for general engineering studies, a simple yet useful PL equation was proposed to calculate v_2 as a mere function of v_1 [12,24,25,32,37]:

$$v_2 = v_1\cdot\left(\frac{h_2}{h_1}\right)^{\alpha} \quad (16)$$

where α is the Hellmann (or friction) exponent, also known as wind shear coefficient (WSC), which depends on the atmospheric stability, wind speed, temperature, land features (and thus z_0) and the height interval, a.o. [4,12,32]. Indeed, Eq. (16) is an engineering formula used to express the degree of stability [12] or amount of turbulence [35] through a single number (α), but has no physical basis.

This formulation implies that there is a single parameter that describes the wind profile at a particular location. For modeling studies this is often assumed to be the case, and is usually constrained by another parameter, such as the surface roughness, that can be defined for that particular location [36]. Furthermore, no information about z_0 features of the area around the anemometer is included in the PL formulation, whose validity is generally limited to the lower atmosphere [12]. According to a number of investigations undertaken at several locations worldwide, WSC may range from 0.40 in urban areas with high buildings to 0.10 over smooth, hard ground, lakes or oceans [35].

4.5.2.4. Determining the value of wind shear coefficient (α). WSC is a highly variable coefficient, often varying from less than 1/7 during the day to more than 1/2 at night over the same terrain [12]. It is to be noted that a 1/7 (0.143) value of WSC is commonly used in many studies worldwide, although in principle it is only appropriate for a smooth terrain with a very low value of z_0 (i.e., 1 cm), or at most for a typical rural terrain, to describe wind profiles up to the first 100 m during near-neutral (adiabatic) conditions [35].

From Eq. (16), α can directly be estimated once records of two wind speeds at different heights (v_1 and v_2) are available [28,30]:

$$\alpha = \frac{\ln(v_2) - \ln(v_1)}{\ln(h_2) - \ln(h_1)} \quad (17)$$

Some researchers have developed methods to calculate the WSC from the parameters in the Log Law. Many researchers, however, feel that these complicated approximations reduce the simplicity and applicability of the general power law and choose values of α that best fit the available wind data [4].

A review of some of the most popular empirical methods for determining representative power law exponents follows.

4.5.2.4.1. Correlation as a function of velocity and height. [38] estimated an exponent for extrapolating the scale factor of the Weibull distribution, and [4] used this estimation as the power law exponent in the following expression:

$$\alpha = \frac{0.37 - 0.0881\cdot\ln(v_1)}{1 - 0.0881\cdot\ln(h_1/10)}. \quad (18)$$

4.5.2.4.2. Correlation based on surface roughness and velocity. Conversely, a number of methods have been developed to estimate α when only surface data are available. For example, according to Spera and Richards [39], α can be calculated as a function of v_1 and z_0 as

$$\alpha = \left(\frac{z_0}{h_1}\right)^{0.2}\cdot\left[1 - 0.55\cdot\log(v_1)\right] \quad (19)$$

Eq. (19) was derived from a number of observations over different locations in the US [12].

4.5.2.4.3. Correlations dependent on surface roughness. Smedman-Högström and Högström [40] proposed a different formulation to calculate α that incorporated z_0 as well as atmospheric stability, which was empirically derived from wind measurements from three 100 m masts in Southern Sweden located over different terrain types (and thus z_0 values):

$$\alpha = c_0 + c_1\cdot\log(z_0) + c_2\cdot[\log(z_0)]^2 \quad (20)$$

where values of stability dependent coefficients c_0, c_1 and c_2 depends on the wind stability class.

[35] proposed the following correlation:

$$\alpha = 0.24 + 0.096\cdot\log(z_0) + 0.016\cdot[\log(z_0)]^2 \quad (21)$$

for 0.001 $m < z_0 < 10$ m.

These, among others, are the most commonly methods used to determine the value of the wind shear coefficient (α).

4.5.2.5. Least-squares method. [41] used the least-squares method to extrapolate 10-m wind measurements to 80 m. The method they used was a least squares fit based on twice-a-day wind profiles from the soundings. For their research, they used surface measurements from 1327 stations and sounding measurements from

87 stations in the U.S. Sounding measurements were available at different altitudes. Approximately 20% of the sounding stations reported measurements at an elevation of $80\,m \pm 20\,m$. Surface stations provide wind speed measurements at a standard elevation of 10 m above the ground. A detailed description of the methodology can be found in [41]. They compared their results with the well-known logarithmic law and power law. Both methods resulted in an average underestimation of the wind speed at 80 m. The power law ($\alpha = 1/7$) led to an average underestimate of annual mean 80-m wind speed of 1.3 m/s. The logarithmic law ($z_0 = 0.01$) underestimated the annual mean 80-m wind speed by 1.7 m/s on average. Both, the power law and the logarithmic law, led to greater underestimates at night than during the day.

4.5.3. Empirical validation of wind speed profile methods

There are a number of authors that have utilized some of the methods previously described in order to determine the wind speed at a certain altitude in a particular area, region or country, and compared the results to empirical data [28,30–33,36,42–44].

[28] compared some of the most commonly used extrapolation methods applied to a case study in a coastal location in Southern Italy, where during 6-year 1-h meteorological dataset, including wind measurements at 10 and 50 m, were registered. They concluded that no analytic formulation for wind speed variation with height may be used which is valid for all stability conditions, and that the integration of different extrapolating methods appears to be a preferable choice. Nevertheless, the power law with the Spera-Richards model proved to be a reliable method to calculate initial estimates of wind speed at hub height, at least under unstable and neutral conditions; these results demonstrate the transportability of the model to a quite rough, coastal site as the one selected in Southern Italy.

[30] determined the accuracy of different wind-shear methods, based on wind data sets of eleven US tall towers over several years (the time step was either 10 min or 1 h). The tall towers were located at different type of terrains (flat, hills with no trees and forests), in order to identify terrain effects. Each tower had wind speed and direction data from at least three different heights, varying from 10 to 123 m, where the highest height was never lower than 75 m in order to represent typical turbine hub-heights. They found that there was no significant difference in performance between the logarithmic and the power law models. The likelihood that either type of model gives a prediction close to the measured value at a site with complex terrain is small. Consequently, using either of these wind-shear models at such sites may result in significantly large inaccuracies for hub-height mean wind speed estimations. Both models, however, accurately predicted the hub-height wind speeds at the three flat sites. Very few of the calculated shear parameters in their analysis at any of the sites were consistent with the typically assumed values for the power law exponents and surface roughness lengths. Even for the flat sites, it was found that the one-seventh power law did not represent the wind-shear. They concluded that tabulated shear parameters and rules of thumb alone should not be relied upon to best represent the wind-shear at a site; analyzing the wind data is an important aspect of accurately predicting the hub-height wind speeds.

[36] recorded wind data from eleven tall towers located in Missouri (US) for one year. Each tower recorded wind data at three different heights, varying from 50 to 147 m, where the highest height was located between 70 and 147 m. The main finding was that the observed winds at each tower were smaller than those presented in the wind map. The discrepancy is most likely to be due to underestimation of the surface roughness and turbulence leading to an overestimation of near-surface wind shear. However, the wind shear, as expressed by the shear parameter was consistently bigger than the 'standard' value of 0.14. The reconciliation of these two apparently contradictory findings is that the shear varies with the height at which it is measured. In wind resource assessment, wind shear is usually observed below 50 m and is tacitly assumed to be constant with height when used to extrapolate winds to higher levels. This wind shear is used to determine the prospects for power production from turbines with hub heights above 80 m, but it should be understood that the wind shear could vary over very small height ranges. Therefore the use of a single value of α at all times will result in potentially large errors in the estimated winds at hub heights, and even the use of the shear observed for each time interval will produce errors in the extrapolated wind because α varies with height. This difficulty in extrapolating 'surface' wind speeds to turbine heights may also contribute to the differences between the observed wind speeds and those presented in wind maps. One way to discriminate some of the competing components of the wind shear is to use the friction velocity, as this does not have the same dependence on wind speed as α. The friction velocity provides a more robust measure for the extrapolation of wind speeds upward. If wind resource assessment uses observations at heights other than the standard 50 m tower then it would be better to use the friction velocity than the shear parameter to perform the extrapolation to turbine levels, as this does not suffer from a speed related bias and is less sensitive to changes in atmospheric conditions.

[43] compiled 9-year wind data at 2 m height by 17 weather stations and 1-year 10 m daily wind speed data from 8 meteorological stations located in Alicante (Southern Spain). They used these data to compare empirical wind data to extrapolation methods (from 2 to 10 m). They concluded that the extrapolation to 10 m using the power law and the wind shear exponent, α (Eqs. (16) and (18)), shows a large underestimation in coastal sites and good values inland, when compared to measurements taken at 10 m.

4.5.4. Method proposed to calculate the wind speed profile

Considering the literature review and the experiences of the different authors, in particular the conclusions drawn by [30,36], it has been decided to use the friction velocity to interpolate and extrapolate wind speeds, since the friction velocity provides a more robust measure for the extrapolation of wind speeds upward [36]. Moreover, the abrupt orography of the Canary Islands does not make it recommendable to use the logarithmic or the power law, since they do not provide good estimations on complex terrains [30].

In order to validate the conclusions drawn by [36] in the Canary Islands, and, therefore, confirm that the selected method for the extrapolation/interpolation is the adequate one for this region, the shear coefficient and the friction velocity have been calculated. The wind atlas data of the Canary Islands (see Table 2), which shows the wind speed at 40, 60 and 80 m, have been used for these calculations.

In order to calculate the shear coefficient the power law has been used, in particular Eq. (17). The calculation of the friction velocity has been done using the logarithmic law, concretely Eq. (15).

The shear coefficient and the friction velocity have been calculated for a sample of locations. Both parameters, the shear coefficient and the friction velocity, have been calculated twice for each location: one value for heights between 40 and 60 m and another value for heights between 60 and 80 m. Table 3 shows the results of these calculations for the Easter part of El Hierro island, as well as the percentage difference between both shear coefficients for each location and between both friction velocities.

Table 3
Shear coefficient and friction velocity, El Hierro island.

UTM_X	UTM_Y	α (40–60 m)	α (60–80 m)	α difference (%)	u (40–60 m)	u (60–80 m)	u difference (%)
211,050	3,073,550	0.228	0.150	34.26	0.612	0.612	0.02
211,350	3,073,350	0.267	0.177	33.51	0.651	0.667	2.44
211,650	3,073,150	0.236	0.157	33.39	0.602	0.612	1.64
211,950	3,072,950	0.220	0.149	32.36	0.582	0.598	2.65
210,750	3,072,450	0.153	0.093	39.12	0.493	0.445	−10.86
211,050	3,072,250	0.170	0.111	34.60	0.513	0.501	−2.48

Table 3 shows that, effectively, as [36] stated, the friction velocity provides a more robust measure for the extrapolation of wind speeds upward. The variations (in percentage terms) between the shear coefficients at different altitudes and between the friction velocities at different altitudes in other islands are similar as the ones for the Easter part of El Hierro island. In this particular case shown in Table 3, the shear coefficient varies around 33% at the two different altitude intervals considered, this change is quite steady for all the islands varying usually from 27% to 40%. The friction velocity is less predictable, varying sometimes in positive terms (increasing values with altitude) and sometimes in negative terms (diminishing values with altitude), but the variation in percentage terms is smaller; the variation for all islands is usually between 0% and 10%, and, in most of the cases, below 5%. Therefore it can be confirmed that, for the analyzed data, the friction velocity is a more steady value. Thus it will be the reference one for the interpolation/extrapolation of wind speed within this study.

The wind speed interpolation/extrapolation method proposed, based on Eq. (15), follows:
For $40 < h < 60$ m:

$$v_h = \left(\frac{u_{40-60}}{K}\right) \cdot \left[\ln\left(\frac{h}{40}\right)\right] + v_{40} \tag{22}$$

For $60 < h < 80$ m:

$$v_h = \left(\frac{u_{60-80}}{K}\right) \cdot \left[\ln\left(\frac{h}{60}\right)\right] + v_{60} \tag{23}$$

For $h > 80$ m:

$$v_h = \left(\frac{u_{60-80}}{K}\right) \cdot \left[\ln\left(\frac{h}{80}\right)\right] + v_{80} \tag{24}$$

For $z < 40$ m, Eq. (13) will be used:

$$v_h = \left(\frac{u_{40-60}}{K}\right) \cdot \left[\ln\left(\frac{h}{z_0}\right)\right] \tag{25}$$

This set of equations (Eqs. (22)–(25)) allows the calculation of the mean wind speed at any height, including the hub height. This set of equations is particularized for the case when the mean wind speed is known at heights 40, 60 and 80 m, but they can be generalized for any other set of different heights.

Table 3 also shows that shear parameters (α) decrease with height, as some authors stated (e.g. [36]), and that the wind shear exponent is different for each site, because its magnitude is influenced by site-specific characteristics, as some authors also stated (e.g. [31]), and that it depends, a.o., on the height interval [4,12,32].

4.6. Extrapolation/interpolation of the shape factor (k) at different altitudes

4.6.1. Shape factor and the reversal height

It has been known for nearly one century that on clear days, the diurnal wind cycle changes phase with height [37,45]. In daytime, efficient boundary layer mixing causes near-equality in wind speeds near the surface and at higher levels. On stable nights, the transfer of air down to the surface is much less, resulting in low surface wind speeds, while simultaneously the wind speeds above the surface inversion increase, because these upper layers lose less momentum to lower layers than in the daytime. For a given level of geostrophic flow, diurnal cycle of wind has, therefore, a nighttime minimum near the surface, while it has a nighttime maximum in the upper planetary boundary layer. In other words, the diurnal cycle changes its phase halfway in the planetary boundary layer, quite distinctively on clear days, less markedly on overcast days. The average height at which this phase reversal occurs is called the reversal height, h_r [46].

A tall mast is needed to observe reversal, the vertical distance between two heights with clearly opposite phases in their diurnal courses is typically > 50 m. A simple profile model shows that, in non-complex terrain, this reversal height varies approximately between 50 m at coasts and 90 m inland [46]. A 200 m mast located at Cabauw (The Netherlands) showed that the seasonal-average reversal height occurs at 80 m [46]. In Oklahoma, the annual-average reversal height lies somewhere around 90 m [47]. At Nauen, in Germany, [37] estimated h_r around 70 m. In Kyoto (Japan) the MU radar (60 to 90 km) measured reversal height at around 84 m in summer and a bit lower in winter [48]. In Cape Kennedy (USA), a site at the cost, the h_r was estimated in 59 m [46].

Frequency distributions of hourly-averaged wind speed can often be well described by the Weibull distribution function. The shape factor k (≥ 1) describes the skewness of the distribution function. For $k \approx 3.5$, the function is nearly symmetrical. Smaller values of k lead to a higher probability of increasing wind speeds. In the case of the Rayleigh distribution, the k-parameter takes a value of 2. The shape factor k has a maximum at the reversal height of the diurnal cycle. When the height decreases, k decreases approximately as a linear function of height [46].

At the surface, the k value is minimal, then k is expected to increase with height to a maximum at reversal height (h_r) and then k should decrease again to some asymptotic value depending on the variability in the troposphere. A simple function that follows this behavior is [46]

$$k - k_s = c_k(h - h_s) \cdot \exp\left(-\frac{(h-h_s)}{(h_r-h_s)}\right) \tag{26}$$

where k_s is the value of k at the surface observation altitude h_s, typically 10 m. The constant c_k takes usually a value near 0.022, which gives satisfactory representations for homogeneous terrain. This function has a k-maximum at height h_r. In the upper planetary boundary layer, it will revert asymptotically to a value close to k_s; maybe not exactly to this value but, according to the limited available data, this approximation will have the right order of magnitude. In Oklahoma (USA), $k_s = 1.72$, and it was found that $k = 1.73$ at $h = 444$ m. In Cabauw (The Nederlands), $k_s = 1.78$, and the local geostrophic wind distribution has a value of $k = 1.82$ [46]. Summing up, there is a tendency of k to converse to k_s at high altitudes. Fig. 2 shows a theoretical representation of the variation of k values with altitude.

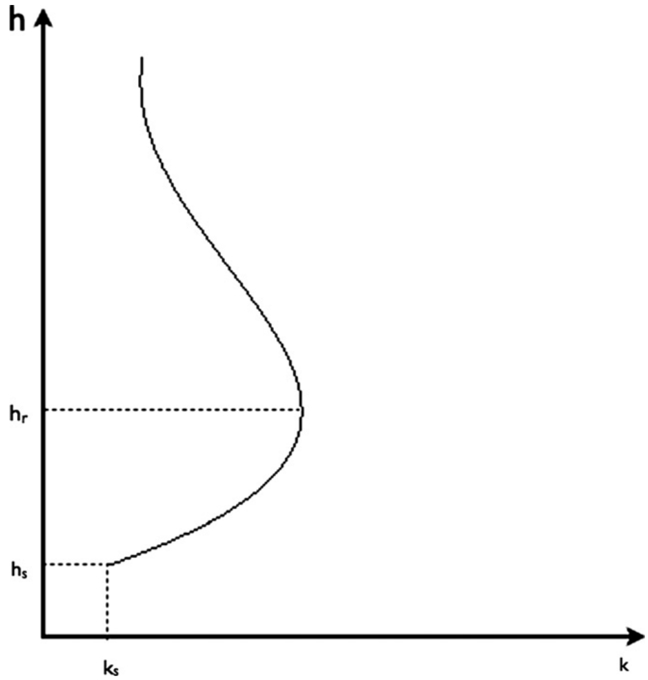


Fig. 2. Variation of *k* values with altitude.

In order to determine the h_r value, it should be taken into account that h_r varies according to geographical conditions. Masts measurements have provided some reversal height values at several places, e.g., in Quickborn (Germany) h_r=70 m, in Vlaardingen (The Nederlands) h_r=63 m, and in the Wallops Island (USA) h_r=52 m. On small islands, h_r-values might be less than 50 m, and at inland sites large h_r-values may be reached if the local diurnal variation of heat flux is big. Experimental data on upper h_r-limits may be difficult to get due to the lack of very tall masts in tropical regions. However, it was found that at Tsumeb (in arid savannah, Namibia), in both dry and wet seasons, the diurnal course of wind speed already had reversed its phase at 120 m [46]. In complex terrain, the reversal height can only be defined very locally and may change by orographic effects. [49] found that $h_r > > 107$ m in the Wyoming mountains (USA).

4.6.2. Method proposed to calculate the shape factor profile

In order to check the conclusions drawn by [46] and to propose a method to be used for the extrapolation/interpolation of the shape factor in the Canary Islands, the wind atlas of the Canary Islands (see Table 2), that shows the shape factor at 40, 60 and 80 m, has been used.

Table 4 shows a sample of shape factor values in the island of Fuerteventura at altitudes of 40, 60 and 80 m as well as the slope of hypothetical shape factor linear functions between 40 and 60 m and between 60 and 80 m.

First at all, it should be notice that the *k* values at 40 m are higher than at 60 m. This is the case for the values shown in Table 4, but it is also the case for almost all the 1905 sites analyzed in the Canary Islands. Only a few sites show *k* values higher at 60 m than at 40 m.

Analyzing these *k* values, one could draw some conclusions on the reversal height. Since the *k* value reaches its highest value at the reverse height and, afterwards, it decreases asymptotically to the k_s value [46], for all locations where k_{40} is higher than k_{60}, which are the majority, the reversal height is located below 60 m, maybe below 50 m or ever lower. These statements are in line with the opinion drawn by [46] that stated that on small islands, z_r-values might be less than 50 m. There are, anyhow, a small group of *k* values where k_{40} is smaller than k_{60}; in these cases the reversal height is located somewhere in between 60 and 80 m, since for all the locations studied the k_{60} value is higher than the k_{80} value.

Table 4
Shape factor in the island of Fuerteventura.

UTM_X	UTM_Y	k_{40}	k_{60}	k_{80}	Slope k_{40-60}	Slope k_{60-80}
595,650	3,130,650	2.656	2.596	2.565	−0.00300	−0.00155
595,650	3,125,050	2.555	2.491	2.477	−0.00320	−0.00070
595,750	3,131,750	2.673	2.614	2.581	−0.00295	−0.00165
595,750	3,126,150	2.592	2.526	2.509	−0.00330	−0.00085
595,850	3,132,850	2.688	2.627	2.595	−0.00305	−0.00160
595,850	3,128,350	2.615	2.552	2.529	−0.00315	−0.00115
595,950	3,130,450	2.651	2.590	2.562	−0.00305	−0.00140
595,950	3,124,850	2.554	2.488	2.476	−0.00330	−0.00060
595,950	3,123,850	2.552	2.488	2.475	−0.00320	−0.00065
596,050	3,131,550	2.670	2.609	2.579	−0.00305	−0.00150
596,150	3,132,650	2.686	2.623	2.594	−0.00315	−0.00145
596,250	3,129,250	2.627	2.564	2.541	−0.00315	−0.00115

Observing Table 4 it can be concluded that the k_{60-80} slope is lower than the k_{40-60} slope; which is also in line with the statement that the *k* value should asymptotically converse to a lower value, k_s (see Fig. 2). After studying these slope values for all locations considered in the Canary Islands, it can be concluded that almost all sites follow this pattern where the k_{60-80} slope is smaller than the k_{40-60} slope. However, for a few sites, the slope of k_{60-80} is higher than the slope of k_{40-60}. This could happen because the reversal height is located somewhere between 40 and 60 m, and the slope between 40 and 60 m first increase, to decrease after the reversal height. For a few sites, the k_{40-60} slope is positive while for all the cases studied the k_{60-80} slope is negative; these are the cases where the reversal height is located between 60 and 80 m.

To determine the equations to be used for the *k* values interpolation/extrapolation, these considerations regarding the reversal height have to be taken into account. To simplify, and due to its high probability, it has been considered that the reversal high is above 40 m in all cases.

Therefore, the interpolation/extrapolation of the shape factor (*k*) is calculated as follows.
For $h<40$, Eq. (26) will be used:

$$k=c_k(h-h_s)\cdot\exp\left(-\frac{(h-h_s)}{(h_r-h_s)}\right)+k_s \tag{27}$$

For $40<h<60$ m, for this interval a linear approximation is considered with a k_{40-60} slope:

$$k=(k_{40-60}\cdot(h-40))+k_{40} \tag{28}$$

For $60<z<80$ m, for this interval a linear approximation is considered with a k_{60-80} slope:

$$k=(k_{60-80}\cdot(h-60))+k_{60} \tag{29}$$

For $h>80$ m, a decreasing slope that asymptotically converse to k_{10} at approximately 450 m will be assumed (according to [46]). For this purpose the *k* values at 10 m for different sites in the Canary Islands have been compiled. Table 5 shows the k_{10} values for a sample of sites in the Canary Islands and its mean value: 1.98. Therefore it will be assume that *k* will converse to this value at a height of 450 m.

The equation that shows this behavior of *k* asymptotically conversing to k_{450} (assuming $k_{450}\cong k_{10}$), considering a linear approximation, is the following:

$$k=\frac{k_{80}-k_{450}}{80-450}\cdot(h-80)+k_{80} \tag{30}$$

Table 5
Values of the shape factor, k, at 10 m: different sites in the Canary Islands.

Site	k_{10}	Altitude	Source
Antigua (FV)	2.28	10	[50]
P. Jandia (FV)	2.44	10	[50]
R. Prieto (GC)	2.13	10	[50]
M. Diablo (GC)	1.94	10	[50]
P. Vargas (GC)	1.98	10	[50]
P. Izquierdo (GC)	2.05	10	[50]
El Rayo (TF)	1.83	10	[50]
Valverde (EH)	1.92	10	[50]
S. Sebastian (LG)	1.89	10	[50]
La Palma	2.26	10	[50]
Granadilla	1.84	10	[51]
Amagro (GC)	1.99	10	[51]
Taca	2.1	10	[51]
LZ airport	1.83	10	[52]
FV airport	2.52	10	[52]
GC airport (Gando)	1.59	10	[52]
TF airport (Sur)	2.27	10	[52]
EH airport	1.41	10	[52]
Mean	1.98		

Substituting the values that are known and assuming that k_{450} takes a value of 1.98, Eq. (30) can be particularized for the Canary Islands as follows:

$$k = \frac{k_{80} - 1.98}{-370} \cdot (h - 80) + k_{80} \quad (31)$$

It has to be highlighted that Eq. (31) has been particularized for the case of the Canary Islands. For a different site, the own values of k at 10 m have to be determined using local wind data.

This set of equations (Eqs. (27)–(31)) allows the calculation of the shape factor at any height, including the hub height. This set of equations is particularized for the case when the shape factor is known at heights 40, 60 and 80 m, but they can be generalized for any other set of different heights, also when the number of available heights is different than three (e.g. two or four).

4.7. Calculation of the wind production

Using the set of equations proposed in this section, the wind energy production can be calculated for any wind turbine just knowing the mean wind speed and the shape factor of the Weibull distribution at any height.

Eq. (11) enables the calculation of the wind energy production in a particular location, using its mean wind speed and shape factor, and for a particular wind turbine, whose power curve is known. The implementation of Eq. (11) requires the mean wind speed and the shape factor at the hub height. Very often these data are not available for the required hub height and they need to be extrapolated from available wind data. If the mean wind speed and shape factor are known for different heights, then one of the Eqs. (22)–(25) can be used to extra/interpolate the wind speed to the desired height, and Eqs. (27)–(31) can be used to extra/interpolate the shape factor to the desired height. Therefore, using a set of three equations, the wind energy production can be easily calculated for any wind turbine at any height.

5. Wind energy cost assessment

5.1. Cost-resources curves: a brief introduction

In general, renewable energy sources are characterized by limited resources, and —if no dynamic costs are considered—costs rise with increased utilization, as e.g., in case of wind power, sites with the best wind conditions will be exploited firstly, and, as a consequence, rising generation costs appear. One tool to describe both costs and potentials represents the static cost-resource curve[1] .

A static cost-resource curve describes the relationship between (categories of) technical available potentials (e.g. wind energy, hydropower, biogas) and the corresponding full utilization cost of this potential at this point-of-time (note that no learning effects are included in static cost-resource curves). On the left side of Fig. 3 a theoretically ideal continuous static cost-resource curve is represented, taking into account that each location is slightly different from each other and, hence, looking at all locations, e.g. for wind energy in a certain geographic area, a continuous curve emerges after these potentials have been classified and sorted in ascending order according to their cost. The stepped function, as shown on the right side of Fig. 3, represents a more practical approach. Thereby, sites with similar economic characteristics (e.g. in case of wind, sites with same range of equivalent hours) are described by one band and, hence, a stepped curve emerges [53].

In summary, cost-resource curves describe the amount of energy that can be provided by a particular technology at a certain cost level [22].

5.2. Annualized wind generation cost

The cost-resource curves calculated in this section represents the wind generation cost assuming current techno-economic parameters. The costs taken into account are the capital investment cost and the exploitation cost.

5.2.1. Investment cost

The total capital cost, or installed capital cost, involves more than just the cost of turbines themselves. The installed investment cost of wind farms, and its corresponding distribution (based on the Spanish market), includes the following items [54,55]:

- Wind turbines: 74%
- Electrical equipment and grid connection: 12%
- Civil work: 9%
- Others: 5%

This distribution is in line with other authors' analysis (e.g. [20]). Regarding the connection to the electrical grid, it has to be taken into account that in Spain wind farm investors assume most of this cost, not the electrical company.

This distribution of the investment cost is also very similar to the one in the U.S. [56]:

- Wind turbines: 80%
- Electrical installation and grid connection: 11%
- Civil work: 5%
- Others: 4%

Even though the major cost component of wind power (the wind turbine) is not site specific, other components like foundations, road costs and grid connection do and these costs may vary considerably depending on the site. Part of grid connection and road construction costs can be considered fixed, since they include roads and power lines between turbines and they do not vary

[1] Other names commonly applied to this term are "supply curves" or "cost curves". Nevertheless, with respect to (renewable) energy sources the term "static cost-resource curves" gives a clear and unambiguous wording [53].

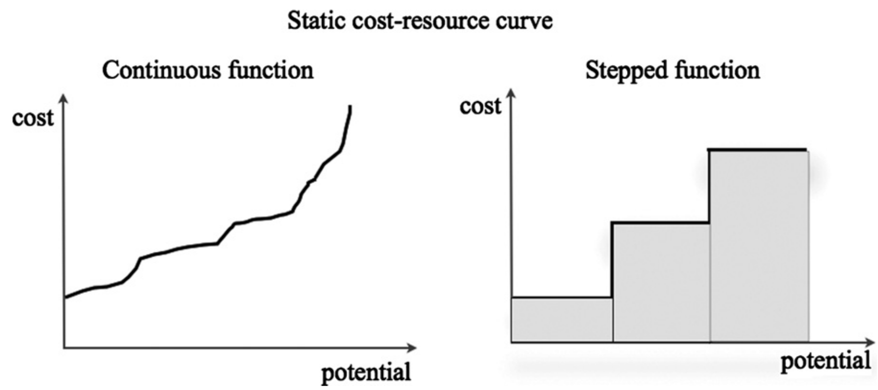


Fig. 3. Static cost-resource curve: continuous (left) and stepped function (right). Based on [53].

much due to wind farm location. Similarly, land costs and foundation installations should not vary significantly between sites.

It is important to bear in mind that in large-scale studies it is difficult to account for site-specific costs, other than wind. For instance, the distribution cost includes the cost of an average evacuation line from the wind farm site to the transport grid, but no provision is made to tailor this cost for one particular site. Similarly, the investment cost assumes common accessibility conditions without considering local accessibility requirements. Therefore, specific distances are not taken into account and average costs for grid enlargement and for access roads construction are considered.

When assuming average wind prices for general studies like this one, it is important to bear in mind which is the average wind project size that is likely to be installed in the targeted area, since prices may vary according to wind farm and wind turbine sizes. There is a steady drop in per-kW average installed costs when moving from projects of 5 MW or less to projects in the 20–50 MW range, varying from 2500 $/kW to 2200 $/kW (2011 values). As project size increases beyond 50 MW, however, there is no evidence of continued economies of scale. Another way to select the average price is by turbine size (rather than by wind farm size), on the theory that a given amount of wind power capacity may be built less expensively using fewer larger turbines as opposed to a larger number of smaller turbines. Installed wind power project costs vary from 2450 $/kW to 2100 $/kW, when changing from wind turbines smaller than 1 MW to wind turbines bigger than 2.5 MW (2011 values) [57].

In 2006, the average investment cost of an installed wind turbine in Spain was 1110 €/kW [54]. Afterwards this cost increased and, in 2010, the average cost of an installed wind turbine in Spain was 1350 €/kW plus an average connection cost of 140 €/kW; which increased the cost of an installed wind turbine up to 1490 €/kW [58]. This last one is the investment cost that has been used within this study. This value is also in line with values expressed by other authors for global market, e.g. [59], who estimated the investment cost of an installed wind turbine in 1380 €/kW.

The increase in turbine prices over this period was caused by several factors, including: increased materials (e.g. steel), energy and labor input prices; a general increase in turbine manufacturer profitability due in part to strong demand growth and turbine and component supply shortages; increased costs for turbine warranty provisions; an up-scaling of turbine size, including hub height and rotor diameter; and complexity increase of the new machines [57,60]

This tendency of prices to rise is not just a local but global effect. After more than two decades of steady reductions of capital cost, wind turbine prices increased during the first years of the XXI century. In the U.S. average wind turbine prices, after hitting a low of roughly 700 $/kW from 2000 to 2002, increased by approximately 800 $/kW (more than 100%) through 2008, rising to an average of more than 1500 $/kW [57]. However, since 2008, wind turbine prices have declined substantially, reflecting a reversal of some of the previously mentioned underlying trends that had earlier pushed prices higher, as well as increased competition among manufacturers and a shift to a buyer's market [57]. In 2011, the capacity-weighted average installed project cost stood at nearly 2100 $/kW, down almost 100 $/kW from the reported average cost in both 2009 and 2010. Moreover, a preliminary estimate of the average installed cost among a small sample of projects that either have been or will be built in 2012 suggests average installed costs decline to around 1900 $/kWh [57]. 1900 $/kWh is equivalent, using 2012 exchange rates, to 1490 €/kWh, which is the investment cost selected for this study.

In Europe, the capital cost of a wind energy project has risen by around 20% over the last years, from 2006. However, the wind capital investment costs are sensibly lower in some emerging markets, notably China. There are also prices differences within the European Union [55].

The reasons behind that spread of values lie on the impact of lower labor costs in some developing countries with manufacturing capacity, the degree of competition in specific markets, the bargaining power of market actors, the national regulation regarding the characteristics of the wind turbine (e.g. existence of strict grid codes), the distance and modality of grid connection (including the possibility to finance all the grid upgrade cost) and the extent of the civil works (which in turn depend on factors such as accessibility and geotechnical conditions of the site) [55]. In this sense, in countries were the development of wind energy has been important, like Spain, Germany or Denmark, it may also occur that the best sites, not just from the resource point of view but also from the accessibility point of view (territorial and electrical), have already been utilized. Therefore, further wind deployment have eventually to be built in less accessible sites or at sites located further away from the electrical grid; making access roads and electrical connections more expensive.

The increase of the investment cost can be explained due to the booming demand of wind energy projects that put pressure on the supply chain. In addition, fast-growing economies such as China are pushing the cost of raw materials upwards. These include steel, copper, lead, cement, aluminum and carbon fiber, all of which are found in the major sub-components of wind turbines. From 2004 to 2007 copper prices rose by over 200%; lead prices increased by 367%; steel prices doubled; aluminum prices increased by 67%; and the prices of acrylonitrile, which is used to produce carbon fiber, increased by 48% over the same period [55].

This increase in the investment cost is not in line with the forecast of the diffusion theory and the learning rate curves.

Circumstantial causes have temporarily influenced the evolution of the investment cost in the opposite way as predicted by these theories. However, as [55] stated, in the long-term, one would expect production costs to go down again, as it has already occurred in the U.S.

5.2.2. Exploitation cost

Next to the purchase and installation of wind turbines, the operation and maintenance cost (O&M) is the most significant cost source. The operation costs include costs as the land rental cost. The maintenance costs include routine checks, periodic maintenance, periodic testing and blade cleaning, among others [4].

The exploitation cost can be classified as: O&M costs and management cost [54]. In 2009, according to a study of the Spanish Wind Association [61], the O&M costs represented approximately 58% of the exploitation costs and the management cost the 42%. The management costs were divided into the following categories [61]:

- Management and administration: 8%
- Insurance, taxes, licenses and canons: 23%
- Electrical and service roads maintenance: 6%
- Others: 5%

[62] studied the O&M cost of more than 5000 machines, concluding that the newer generation of WTs has lower repair and maintenance costs in comparison to the older generation. Specifically, the older WTs (sized from 25 to 150 kW) had annual maintenance costs averaging about 3% of the turbines capital cost. For the newer machines, the estimated annual O&M costs range from 1.5% to 2% of the capital cost. [57] show similar conclusions: Berkeley Lab has compiled O&M cost data for 133 installed wind power projects in the United States, totaling 7965 MW of capacity, with commercial operation dates of 1982 through 2010. The average O&M cost dropped from 40 $/MWh in 1982 to 10 $/MWh in 2010.

However, this tendency seems to have changed slightly in the last years, at least in some countries. [57] estimated capacity-weighted average O&M costs in 65 $/kW-a for projects constructed in the 1980s, dropping to 54 $/kW-a for projects constructed in the 1990s, and to 28 $/kW-a for projects constructed since 2000. Somewhat consistent with these observed O&M costs, [57] reports the cost of 5-year full-service O&M contracts at 30–48 $/kW-a (representing approximately 1.5% of the investment cost in 2011).

In Spain the exploitation cost rose from 16 €/kW-a in 2006 [54] to approximately 19.5 €/kW-a in 2010 [58]. This increase in the exploitation cost is due to the increase of the management cost, forecasting, real time management, remote-control and also because new facilities tend to be more complex and licenses and canons tend to increase [60].

The exploitation cost in 2010 in Spain (19.5 €/kW-a) represented approx. 1.3% of the investment cost corresponding to that year. This percentage of the investment cost is the one proposed in this study for the exploitation cost.

5.2.3. Lifetime of the system

It is a common practice to equal the design lifetime to the economic lifetime of an energy system [4]. In Europe, a period of 20 years is often assumed for the economic assessment of wind energy systems [63]. This follows the recommendations of [62], who stated that a 20-year design lifetime is a useful economic compromise to guide engineers who develop components for wind turbines. Exceptionally other authors have utilized other lifetime periods, e.g. 15 years [64], but this value of 20 years lifetime is in line with many other authors [9,20,22,55,65,66]. 20 years seems to be the standard “business” lifetime, which is the time bankers amortize loans over. However, experience show that most wind farms could last 30 years or longer. Therefore, 30 years is a reasonable period for the economic or real lifetime of the turbine. Thus, the wind electricity costs are calculated using a lifetime period of 20 and 30 years.

5.2.4. Wind electricity generation cost

Table 5 shows the techno-economic parameters proposed to calculate the wind electricity generation costs.

The wind electricity generation cost (€/kWh) can be annualized using

$$C_{x,y} = \frac{a \cdot I + C_{O\&M}}{h_{eq(x,y)}} \tag{32}$$

where $C_{x,y}$: wind electricity generation cost (€/kWh) in location x, y; a: annuity factor, given by: $a = r/1-(1+r)^{-LT}$; I: investment cost (€/kW); r: interest rate; in this case 6%. For this type of projects [67] suggested a value between 4% and 6% for the nominal discount rate and [68] a 5% for the Euro area and the USA (equivalent to an interest rate of 5.2%). The value of 6% has been set to be on the conservative side (note that this interest rate will lead to higher generation costs). Other authors have used higher interest rates, e.g. ([9]: 10%; [65]: 9%); LT: lifetime (a); $C_{O\&M}$: operation and maintenance cost (€/kW · a); $h_{eq(x,y)}$: annual equivalent hours at location x, y (h/a).

The annual equivalent hours can be calculated as follows:

$$h_{eq(x,y)} = \frac{E_{x,y}}{WT_{power}} \tag{33}$$

where $E_{x,y}$=annual energy production at location (x,y), in MWh per year; WT_{power}: power of the selected wind turbine, in MW.

Table 7 shows, as an example, wind generation costs at some of the worst and the best sites in El Hierro island, considering a hub height of 80 m, and two different lifetimes: 20 and 30 years (Table 7).

5.3. Cost resources curves

Once the annualized generation cost have been calculated for a whole area (e.g. an island, a region, a country, municipality or just any selected area), the cost resource-curve can be plotted. The annualized generation cost has been calculated for all sites in each of the Canary Islands where windfarms can be places. Fig. 4 shows the results for El Hierro island, considering a lifetime of 20 and 30 years.

The generation costs obtained for the Canary Islands can be compared with the costs obtained in other studies. [65] calculated the wind generation cost for Spain concluding that the lowest cost, in areas with very good wind resources, was around 4 c€/kWh. For a production level of 300 TWh/a, the marginal cost was around 8.5 c€/kWh, occupying an area equivalent to 6.9% of the Spanish surface: 34,000 km^2 (the electricity demand in Spain in 2011 was 270 TWh [69]). [55] researched the wind generation costs in Europe, concluding that the generation cost per kWh of an onshore wind farm ranges from 4.5 to 8.7 c€/kWh.

Table 6
Techno-economic parameters of wind on-shore for cost-resource curve assestment (2010).

Technology	Investment (I_0)	Exploitation cost	Life-time
	[€/kW]	[€/(kWa)]	[a]
Wind on-shore	1490	1.3% · I_0	30 (and 20 years: sensitivity analysis)

Table 7
Wind generation cost:sample in El Hierro island

UTM X	UTM Y	V_{80} (m/s)	Production$_{80}$ (MWh/a)	h_{eq} (80)	Cost$_{80}$ (c€/kWh) LT: 20	Cost$_{80}$ (c€/kWh) LT: 30
214,050	3,077,950	8.9	9349	4674	3.2	2.7
210,750	3,072,450	8.6	8946	4473	3.3	2.8
214,350	3,077,750	8.2	8292	4146	3.6	3.1
213,850	3,079,450	7.4	6989	3495	4.3	3.6
211,950	3,072,950	7.3	6810	3405	4.4	3.8
208,950	3,082,750	6.1	4543	2271	6.6	5.6
208,950	3,081,550	6.0	4203	2101	7.1	6.1
210,150	3,081,950	5.8	3943	1971	7.6	6.5
209,850	3,082,150	5.5	3407	1703	8.8	7.5

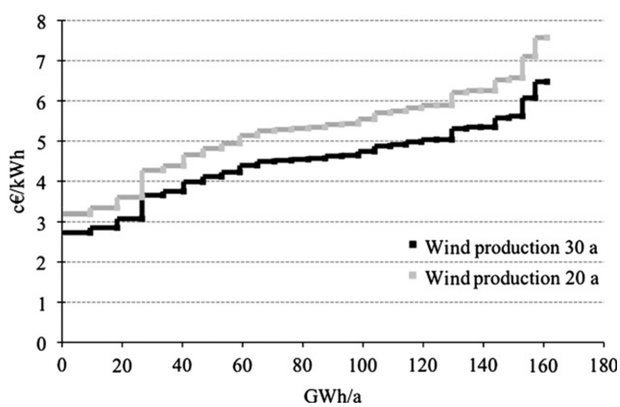


Fig. 4. Wind cost resource-curve for El Hierro island.

Because of the good wind resources in the Canary Islands, the generation costs are lower than in Spain. For example, the electricity demand in El Hierro island during 2011 was 44.5 GWh. Fig. 4 shows the wind generation cost in the island, showing that the marginal cost for 47 GWh is 4.8 c€/kWh; which can be produced by 12 MW. This cost represents only the wind generation cost, excluding integration costs, e.g. storage, grid management, etc. The lowest generation cost in this island is 3.2 c€/kWh.

6. Conclusions

The aim of the methodology proposed is to calculate the techno-economical wind energy production in a given area, just having as input data the mean wind speed and the shape factor of the Weibull distribution at any height or, even, just only the mean wind speed. To locate the wind turbines, one of the most important issues to be taken into account is the wake effect, which conditions the wind farm configuration. The wake effect is a complex issue, still under research, since a lot of parameters influence this effect and, therefore, the optimal wind farm configuration. The wind farm configuration depends on the economical criterion selected. One criterion is to minimize the wind production cost, for this purpose the array efficiency sought is 100%, but this increases the distances among wind turbines and, therefore, reduces the number of machines that can be installed. Another criterion is to maximize the incomes within a given area; in this case the wind turbines may be placed closer, reducing the array efficiency but increasing the wind production per area. The first criterion is the one selected in this study, which led to an array efficiency of nearly 100% and to a wind farm configuration of $12D \times 4D$ (D: rotor diameter).

The selection of the reference wind turbine to be used is also critical since, among others, the rotor diameter conditions the wind farm configuration and the tower height remarkably influences the energy production. Once all the wind turbines are placed and the tower height for the reference turbine is selected, the energy production can be calculated. The wind production is calculated using the data provided by the power curve of the selected wind turbine and the mean wind speed and shape factor of the Weibull distribution at the hub height.

To calculate the energy production at hub height the mean wind speed and the Weibull shape factor have to be interpolated and/or extrapolated. There is still a lot of research on going in order to determine the optimal method to inter/extrapolate wind speeds and the shape factor. In this study the methodology considered as the most accurate to inter/extrapolate the wind speed has been based on the friction velocity; on the one hand, due to the abrupt orography of the region considered, since the logarithmic and power law models provide inaccurate predictions at sites with complex terrain [30] and, on the other hand, because the friction velocity provides a more robust measure for the extrapolation of wind speeds upward [36]. For the sites studied in the Canary Islands, the friction velocity at 40–60 m compared to the one at 60–80 m, was quite unpredictable, increasing with the height in some cases but decreasing in other cases; being the average variation in percentage terms smaller than 5%. In contrast, the mean variation of the wind shear coefficient at the same heights was around 33%, decreasing in all cases with the height. Therefore it can be confirmed that, for the analyzed data, the friction velocity is a more steady value.

In order to inter/extrapolate the Weibull shape factor, the reversal height has been taken into account. At the surface the value of the shape factor (k) is minimal, then k increases with height reaching its maximum at the reversal height (h_r) and then k decreases asymptotically to a value close to its minimal [46]. The shape factor (k) values and their slopes have been analyzed for 1905 sites in the Canary Islands, concluding that, for almost all sites studied, the reversal height is located below 60 m. A set of equations has been proposed to calculate the mean wind speed and the shape factor at the hub height based on the mean wind speed and shape factor at three different heights. This set of equations can be generalized for any different heights. Therefore, using a set of three equations, the wind energy production can be easily calculated for any wind turbine at any height.

A simple method for the calculation of the annualized wind generation cost (c€/kWh) for a given area has been proposed, based on investment and operation and maintenance costs in 2010. The analysis of the wind cost evolution shows that, between 2006 and 2010, the wind investment cost in Spain increased more than 20% due to several reasons (from raw materials cost increase to higher integration costs, a.o.). This increase in the investment cost is not in line with the diffusion theory and the learning rate curves. Circumstantial causes have temporarily influenced the evolution of the investment cost in the opposite way as predicted by these theories. However, in the long-term, one would expect production costs to go down again.

The results of the economical assessment show that the wind generation cost in some of the best sites of the Canary Islands are a bit lower than 3 c€/kWh. The marginal wind generation cost (that equals the demand) in El Hierro island goes up to nearly 5 c€/kWh.

References

[1] World Wind Energy Association, Report 2011; 2012.
[2] European Wind Energy Association, wind in power. European Statistics; 2012.
[3] European Wind Energy Association, Pure Power. Wind energy targets for 2020 and 2030; 2009.

[4] Manwell JF, McGowan JG, Rogers AL. Wind energy explained. theory, design and application. 2nd ed. Chichester, UK: Wiley; 2009.
[5] Mathew S. Wind energy: fundamentals, resource analysis and economics. The Netherlands: Springer Verlag; 2006.
[6] Hau E. Wind turbines: fundamentals, technologies, application, economics. Germany: Springer Verlag; 2006.
[7] Archer CL, Jacobson MZ. Evaluation of global wind power. Journal Geophysical Resources 2005;110:D12110.
[8] Wen J, Zheng Y, Donghan F. A review on reliability assessment for wind power. Renewable and Sustainable Energy Reviews 2009;13:2485–94.
[9] Hoogwijk MM, On the global and regional potential of renewable energy sources, Universiteit Utrecht, Faculteit Scheikunde; 2004.
[10] Grubb MJ, Meyer NL. In: Johansson TB, Burnham L, editors. Wind energy: resources, systems and regional strategies. Washington (United Stated): Island Pr; 1993.
[11] Rodríguez Amenedo JL, JC Burgos Díaz, Gómez S Arnalte. Sistemas Eólicos De Producción De Energía Eléctrica. Rueda, Madrid, 2003.
[12] Spera DA Wind turbine technology. 2nd ed; 2009.
[13] Jacobson MZ, Archer CL. Saturation wind power potential and its implications for wind energy. Proceedings of the National Academy of Sciences 2012;109: 15679–84.
[14] Frandsen ST. Turbulence and turbulence-generated structural loading in wind turbine clusters. Roskilde, Denmark: Risø National Laboratory; 2007.
[15] Lissaman PBS, Gyatt G, Zalay A, Numeric-modeling sensitivity analysis of the performance of wind turbine arrays; 1982.
[16] Aytun Ozturk U, Norman BA. Heuristic methods for wind energy conversion system positioning. Electric Power Systems Research 2004;70:179–85.
[17] Mosetti G, Poloni C, Diviacco B. Optimization of wind turbine positioning in large windfarms by means of a genetic algorithm. Journal of Wind Engineering and Industrial Aerodynamics 1994;51:105–16.
[18] Grady S, Hussaini M, Abdullah M. Placement of wind turbines using genetic algorithms. Renewable Energy 2005;30:259–70.
[19] Emami A, Noghreh P. New approach on optimization in placement of wind turbines within wind farm by genetic algorithms. Renewable Energy 2010;35:1559–64.
[20] Serrano González J, Gonzalez Rodriguez AG, Castro Mora J, Riquelme-Santos J, Burgos Payan M. Optimization of wind farm turbines layout using an evolutive algorithm. Renewable Energy 2010;35:1671–81.
[21] van Haaren R, Fthenakis V. GIS-based wind farm site selection using spatial multi-criteria analysis (SMCA): evaluating the case for New York State. Renewable and Sustainable Energy Reviews 2011;15:3332–40.
[22] Held A, Modelling the future development of renewable energy technologies in the European electricity sector using agent-based simulation; 2011.
[23] Da Rosa AV. Fundamentals of renewable energy processes. 2nd ed. USA: Academic Press; 2009.
[24] Davenport AG. The relationship of wind structure to wind loading. Teddington, Middlesex: National Physical Laboratory; 1963.
[25] Justus C, Hargraves W, Yalcin A. Nationwide assessment of potential output from wind-powered generators. Journal of Applied Meteorology 1976;15: 673–8.
[26] Carta JA, Calero R, Colmenar A, Castro MA. Centrales De Energías Renovables: Generación Eléctrica Con Energías. Madrid: Pearson. Prentice Hill; 2009.
[27] Masters GM. Renewable and efficient electric power systems. New Jersey - USA: Wiley-IEEE Press; 2004.
[28] Gualtieri G, Secci S. Comparing methods to calculate atmospheric stability-dependent wind speed profiles: a case study on coastal location. Renewable Energy 2011.
[29] Yeh T, Wang L. A study on generator capacity for wind turbines under various tower heights and rated wind speeds using Weibull distribution. IEEE Transactions on Energy Conversion 2008;23:592–602.
[30] Elkinton MR, Rogers AL, McGowan JG. An investigation of wind-shear models and experimental data trends for different terrains. Wind Engineering 2006;30:341–50.
[31] Singh S, Bhatti TS, Kothari DP. A review of wind-resource-assessment technology. Journal of Energy Engineering 2006:8–14.
[32] Bañuelos-Ruedas F, Angeles-Camacho C, Rios-Marcuello S. Analysis and validation of the methodology used in the extrapolation of wind speed data at different heights. Renewable and Sustainable Energy Reviews 2010;14: 2383–91.
[33] Farrugia RN. The wind shear exponent in a Mediterranean island climate. Renewable Energy 2003;28:647–53.
[34] Monin A, Obukhov A. Dimensionless characteristics of turbulence in the surface layer. Akademiya Nauk Kazakhskoy SSR Geofisica Trudy 1954;24: 151–63.
[35] Counihan J. Adiabatic atmospheric boundary layers: a review and analysis of data collected from the period 1880–1972. Atmospheric Environment 1975;9:871–905.
[36] Fox NI. A tall tower study of Missouri winds. Renewable Energy 2011;36: 330–7.
[37] Hellmann G. Über Die Bewegung Der Luft in Den Untersten Schichten Der Atmosphäre, Kgl. Akademie der Wissenschaften [G.] Reimer; 1914.
[38] Justus C. Winds and wind system performance. Philadelphia; 1978.
[39] D Spera, T Richards. Modified power law equations for vertical wind profiles. In: Proceedings of the conference and workshop on wind energy characteristics and wind energy siting; 1979.
[40] Smedman-Hogstrom AS, Hogstrom U. A practical method for determining wind frequency distributions for the lowest 200 m from routine meteorological data(for windpower studies). Journal of Applied Meteorology 1978;17: 942–54.
[41] Archer CL, Jacobson MZ. Spatial and temporal distributions of US winds and wind power at 80 m derived from measurements. Journal of Geophysical Research 2003;108:4289.
[42] Elamouri M, Ben Amar F. Wind energy potential in Tunisia. Renewable Energy 2008;33:758–68.
[43] Cabello M, Orza J. Wind speed analysis in the province of Alicante, Spain. Potential for small-scale wind turbines. Renewable and Sustainable Energy Reviews 2010;14:3185–91.
[44] Mostafaeipour A. Feasibility study of harnessing wind energy for turbine installation in province of Yazd in Iran. Renewable and Sustainable Energy Reviews 2010;14:93–111.
[45] Peppler A. Windmessungen auf dem Eilveser Funkenturm. Beitraege zur Physik der Atmosphaere 1921;9:114–29.
[46] Wieringa J. Shapes of annual frequency distributions of wind speed observed on high meteorological masts. Boundary-Layer Meteorological 1989;47:85–110.
[47] Crawford KC, Hudson HR. The diurnal wind variation in the lowest 1500 ft in Central Oklahoma. June 1966–May 1967. Journal of Applied Meteorology 1973;12:127–32.
[48] Nakamura T, Tsuda T, Fukao S. Mean winds at 60–90 km observed with the MU radar (35°N). Journal of Atmospheric and Terrestrial Physics 1996;58:655–60.
[49] Martner BE, Marwitz J. Wind characteristics in southern Wyoming. Journal of Applied Meteorology 1982;21:1815–27.
[50] Carta JA, Ramírez P. Analysis of two-component mixture Weibull statistics for estimation of wind speed distributions. Renewable Energy 2007;32:518–31.
[51] Carta JA, Ramírez P, Velázquez S. A review of wind speed probability distributions used in wind energy analysis: case studies in the Canary Islands. Renewable and Sustainable Energy Reviews 2009;13:933–55.
[52] Carta JA, Velázquez S. A new probabilistic method to estimate the long-term wind speed characteristics at a potential wind energy conversion site. Energy 2011;36:2671–85.
[53] Resch G. Dynamic cost-resource curves for electricity from renewable energy sources and their application in energy policy assessment; 2005.
[54] AEE, Eólica 07. Todos los datos, análisis y estadísticas del sector eólico; 2007.
[55] Blanco MI. The economics of wind energy. Renewable and Sustainable Energy Reviews 2009;13:1372–82.
[56] Jacobson MZ, Masters GM. Exploiting wind versus coal. Science 2001;293 [1438–1438].
[57] Wiser R, Bolinger M. Wind Technologies Market Report, 2011 Wind Technologies Market Report; 2012.
[58] Deloitte, Estudio del impacto macroeconómico del sector eólico en España 2010; 2010.
[59] Prideaux E, Harrison L. Drivers for growth stronger than ever. Wind Power Monthly 2009;25:74–6.
[60] Intermoney Energía, Análisis y diagnóstico de la generación eólica en España; 2006.
[61] AEE, Eólica 9. Todos los datos, análisis y estadísticas del sector eólico; 2009.
[62] Danish Wind Industry Association, Guided Tour on Wind Energy; 2006.
[63] World Energy Council, Renewable Energy Resources: Opportunities and Constraints 1990–2020; 1993.
[64] Voivontas D, Assimacopoulos D, Mourelatos A, Corominas J. Evaluation of renewable energy potential using a GIS decision support system. Renewable Energy 1998;13:333–44.
[65] Fueyo N, Sanz Y, Rodrigues M, Montañés C, Dopazo C. The use of cost-generation curves for the analysis of wind electricity costs in Spain. Applied Energy 2011;88:733–40.
[66] Kaltschmitt M, Streicher W, Wiese A. Renewable energy: technology, economics and environment. Germany: Springer Verlag; 2007.
[67] Mir P. Economía De La Generación Fotovoltaica. Milenio, Lleida; 2009.
[68] Nofuentes G, Aguilera J, Muñoz F. Tools for the profitability analysis of grid-connected photovoltaics. Progress in Photovoltaics: Research and Applications 2002;10:555–70.
[69] Red Eléctrica de España, Red Eléctrica de España web page; 2012.